

Intensity and Shape of the X-Ray-Edge Singularity

Pierre Longe*

Institut de Physique, Université de Liège, Sart-Tilman, B-4000 Liège, Belgium

(Received 26 January 1973)

The singularity at the Fermi edge in the soft-x-ray spectra of metals is known to be described by a factor $|\xi_0/\epsilon|^{\alpha}$ multiplying the one-electron intensity. Using a separable potential, Nozières and deDominicis showed that α is a function of the Fermi-electron phase shifts. However, ξ_0 , treated until now as a constant, has not yet been derived. We extend the above factor to other frequencies, writing it in the form $G(\epsilon)\xi(\epsilon)/\epsilon^{\alpha}$. Using simplified diagrams we can introduce a realistic potential and orthogonalized plane waves and we determine $G(\epsilon)$ and $\xi(\epsilon)$ in a range of about 3 eV from the edge. The calculations are applied to $\text{NaL}_{2,3}$, LiK , and BeK bands. The factor $G(\epsilon)$, related to the open-line part of the problem, presents a singularity in the slope at $\epsilon = 0$. This fact, important in the K bands, was not realized before. However, the edge singularity does not appear to be strong enough to explain the premature peak in the K -emission bands. The p -scattering resonance discussed by Allotey is probably dominant here.

I. INTRODUCTION

The expression describing the edge singularity of the soft-x-ray band spectra of metals was derived four years ago by Nozières and de Dominicis¹ (hereafter quoted as ND). This expression has the form of a power law as conjectured by Mahan²:

$$I_1(\omega) = I_1^0(\omega) G_0 (\xi_0 / |\omega - \omega_0|)^{\alpha_1}, \quad (1)$$

with

$$\alpha_1 = 2\delta_1/\pi - 2 \sum_{l'=0}^{\infty} (2l'+1)(\delta_{l'}/\pi)^2. \quad (2)$$

The δ_l 's are the electron phase shifts at the Fermi level, the scatterer being the localized core hole involved in the x-ray transition; $I_1^0(\omega)$ is the one-electron transition intensity and ω_0 is the Fermi-edge frequency.

Since then, a number of papers³ were devoted to the study of this singularity where various secondary effects neglected by ND are investigated, namely, the temperature dependence,⁴ the effects of the many-body correlations,⁵ the lattice relaxation,⁶ and the hole recoil.⁷ These effects are small and therefore the simple model used by ND may be considered quite satisfactory. In this model the conduction electrons interact individually with the core hole through an effective static potential switched suddenly at the moment of the x-ray transition.

However, Eq. (1) is valid only in the neighborhood of the Fermi edge. Moreover it contains two unknown constant factors: ξ_0 , related to the core-hole potential, and G_0 , related to the open-line part of the problem. Actually these factors are not constant but depend on the frequency. A better way to write Eq. (1) would be

$$I_1(\omega) = I_1^0(\omega) G(\omega) [\xi(\omega) / |\omega - \omega_0|]^{\alpha_1}, \quad (3)$$

with $G(\omega_0) = G_0$ and $\xi(\omega_0) = \xi_0$. The aim of this paper

is to determine all these functions, especially in the Fermi-edge region.

It is not the first time that the shape of the band spectra of metals described by the one-electron model is questioned. Previously attention was paid to the low-energy features in emission, namely, the tailing,⁸ which modifies the one-electron band shapes proposed by Skinner *et al.*⁹ In his model the total intensity is given by $I_1^0(\omega)$, which is approximately proportional to $\omega^{(l+1)/2}$ for the simple metals (energy $\omega = 0$ is ascribed to the bottom of the emission band). The contribution of this tailing to the total emission intensity, however, is weak. This tailing is due to the electron interactions, which also play a role inside the bands. This role, investigated in Ref. 5, may be considered to consist of two parts. First, the static part of the effective interaction of the conduction electrons with the core hole gives rise to the edge singularity and affects the whole band in emission and absorption. Second, the dynamical part of this interaction and the interactions between the conduction electrons (correlations) give a contribution which appears as a more or less constant background, contrary to what happens with the static part of the core-hole interaction. The tailing in the emission spectra chiefly appears as an extension of this background. It was estimated by the author in collaboration with Bergersen and Brouers⁵ in a first-order calculation (see Fig. 1). It depends weakly on the core-hole structure (treated in Ref. 5 as a point charge) and, in fact, does not modify strongly the general shape of the bands.

The situation is quite different concerning the static core-hole-electron interaction. In the edge region, where it gives rise to the singularity, an expansion of the interaction in a few terms is not suitable. Moreover, as was shown previously,¹⁰ the open-line part of the problem is very sensitive

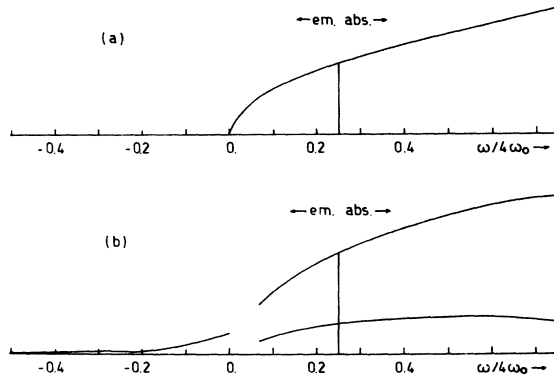


FIG. 1. Emission and absorption $L_{2,3}$ band of Na, according to Ref. 5, (a) in the one electron theory and (b) when account is taken of the electron-electron interactions and of the dynamical part of the interaction with the core hole (treated as a point impurity). These effects are calculated in a first-order theory (which fails in the small region $\omega \gtrsim 0$). The effect of the static part of the hole interaction, namely the edge singularity, is not represented here [see Fig. 8(a)].

to the core-hole structure. In fact, up to now, only the exponent α_l of (3) is known. It is given by the general ND expression (2). Ausman and Glick¹¹ estimated it for Li and Na. Further we shall discuss their values and extend their results to other metals.

In this paper, however, we shall mainly be interested in determining $\xi(\omega)$ and $G(\omega)$. In ND, $G(\omega)$ is an undetermined constant and $\xi(\omega_0) = \xi_0$ is assumed to be of the order of the Fermi energy ω_0 . In other words, ND calculations do not depart from the Fermi edge. Moreover, the problem of calculating the absolute intensity, solved by Skinner in the one-electron model, appears again.

This latter problem, often let aside is, however, important. Presently, the absolute intensity is still considered as hard to measure, but we would like to point out recent experiments performed by Kerr Del Grande and Oliver¹² to determine such intensities in absorption. Comparison of intensities between neighboring emission bands with different l is also possible experimentally and would require the knowledge of the constant factors in (1). From a more theoretical point of view, there is an important question. Is it correct to interpret the band-spectra intensities as a simple product of a one-electron oscillator strength and a density of states? On the other hand, in some applications one may have to compute intensities by means of a perturbative expansion of the type

$$I_l(\omega) \propto I_l^0(\omega) [1 + \alpha_l \ln(\xi_0/|\omega - \omega_0|)] ,$$

valid at some distance from the Fermi edge. In such calculations, ξ_0 must be known even if one is

not concerned with the absolute intensity, whereas in Eq. (1), ξ_0 appears only in a scaling factor, $G_0 \xi_0^{\alpha_l}$.

Another problem, considered in this paper, is the ω dependence of $\xi(\omega)$ and $G(\omega)$. The method we will use gives the best results at the Fermi edge. However it may be extended safely at some distance from this edge. In emission, it covers practically all the band, except the tailing region where the methods of Ref. 8 give better results. The ω dependence is particularly important for $\alpha_l < 0$ (K bands), where one has to determine the position of an intensity maximum in the emission bands. The problem of the premature peak of the lithium- K -emission band is an old problem. Presently it has two possible explanations: first in terms of the electron-hole p -scattering resonance considered by Allotey,¹³ and more recently in terms of the edge singularity which is a rounding-off effect when $\alpha_l < 0$. The problem is to know which of these two effects is dominant. We will examine this problem for Li and Be. The ω dependence in (3) may also be important not only for K bands but also for $L_{2,3}$ bands, where $\alpha_l (= \alpha_0)$ has its largest absolute value.

In Sec. II we give the general formulation of the problem, based on the two-Hamiltonian model. Attention is paid to the introduction of a nonseparable potential, i. e., a realistic potential, which will be used throughout our calculations. First, in Sec. III, we treat the closed-loop part of the problem. We show that the two vertex loops provide the exponent (2) as a function of the Born-approximation phase shifts. In Sec. IV, using various arguments, we show that these phase shifts give satisfactory results for the usual metal densities. In Sec. V the open-line part of the problem is treated. Up to this section, the calculations are performed by describing the core-hole interaction with the help of a pseudopotential; the effects of various model potentials are also considered. In Sec. VI the orthogonalized-plane-wave (OPW) method is directly introduced and applied to the $L_{2,3}$ band of Na and to the K bands of Li and Be. The results are discussed in Sec. VII.

II. FORMULATION OF THE PROBLEM

The x-ray emission/absorption intensity is given by

$$I_l(\omega) = \text{Re} \int_0^\infty ds e^{\pi i \omega s} F_l(s) \quad (4)$$

with

$$F_l(s) = \frac{1}{2l+1} \sum_{m=-l}^l \sum_{\vec{k}, \vec{k}'} \bar{W}_{lm}(\vec{k}') W_{lm}(\vec{k}) M_{\vec{k}\vec{k}'}(s) . \quad (5)$$

Here and in what follows the upper signs are related to emission and the lower signs to absorption.

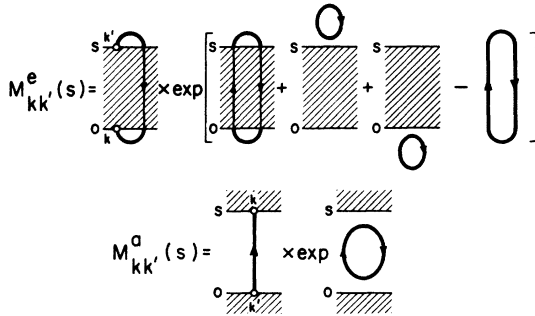


FIG. 2. Diagrammatic representation of Eqs. (7) in the emission and in the absorption case. The core state is occupied during the shaded time intervals. The open circles represent the interaction with the radiation field.

The energies k^2 and frequencies ω are measured from the bottom of the conduction band;

$$W_{lm}(\vec{k}) = k^l h_l(\vec{k}) Y_m^l(\hat{k}) \quad (6)$$

[with $h_l(0) \neq 0$] represents the matrix element of the x-ray transition between the conduction state k and the core state; l and m are related to the total angular momentum of the core state and the x-ray photon; one averages over the $2l+1$ degenerate states. The propagator $M_{kk'}^{\pm}(s)$ may be written⁵ as

$$M_{kk'}^{\pm}(s) = \frac{\langle |U'(\infty, s) a_{\vec{k}}^{\pm}(s) U(s, 0) a_{\vec{k}}(0) U'(0, -\infty)| \rangle}{\langle |U'(\infty, -\infty)| \rangle} \quad (7a)$$

in the emission case, and as

$$M_{kk'}^{\pm}(s) = \frac{\langle |U(\infty, s) a_{\vec{k}}^{\pm}(s) U'(s, 0) a_{\vec{k}}^{\pm}(0) U(0, -\infty)| \rangle}{\langle |U'(\infty, -\infty)| \rangle} \quad (7b)$$

in the absorption case. We use the two-Hamiltonian model which is now standard for this problem.^{1,5} When the core state is vacant, the evolution of the system is described by the operator U' , related to an electron gas interacting with the localized charge $+e$. When the core state is occupied, the operator U is used, which is related to the usual homogeneous electron gas. The general diagrams describing $M_{kk'}^{\pm}(s)$ are given in Fig. 2. In the absorption case, the ND diagrams are easily recognized. The emission case is somewhat more sophisticated because we consider that the scatterer is present in the *initial* state, contrary to the ND model, where it acts in the final state both in the emission and absorption cases. This convention, which we used before,⁵ allows us to describe the one-electron states by nonscattered Bloch waves in both cases. However, a relevant vacuum contribution coming from the renormalizing denominator of (7a) must be taken into account. This contribution is represented by the last term between the brackets in Fig. 2(a). The shaded in-

tervals in Fig. 2 are those during which the scatterer does not operate. The thin and heavy lines are defined as in Fig. 1 of ND: The thin line denotes the free-electron propagator, the heavy line the renormalized propagator when the scatterer is present.

The exponent (2) contains two terms. The first one, $2\delta_1/\pi$, comes from the open-line contribution of Fig. 1 and the second one,

$$\sigma_0 = -2 \sum_{l'=0}^{\infty} (2l'+1)(\delta_{1l'}/\pi)^2, \quad (8)$$

comes from the closed-loop contribution. This result was obtained by ND and other authors¹⁴ by replacing the realistic core-hole potential by a separable potential. This approximation allows one to establish the power law with a correct exponent, but fails however in the calculation of $\xi(\omega)$. Such a calculation requires a *realistic potential*. It is what we do, but we will be compelled to make other approximations. In fact, we will use two types of approximations. One applies to the closed-loop part of Fig. 2, the other to the open-loop part, and the validity of these will be checked by appealing to the ND expressions (1) and (2).

III. CLOSED-LOOP CONTRIBUTION

Concerning the closed-loop part, we will only take into account the lowest-order significant loops, which are the two vertex loops. Such an approximation can be justified by showing that it leads to quite satisfactory δ_1 's. Let us consider first the case where only one loop accompanies the x-ray process and let us represent this single-loop contribution by C_{1oop} . In Fig. 2, it appears in a factor $e^{C_{1oop}}$ which is then approximated by $(1 + C_{1oop})$. Using the diagram rules stated in Appendix C, Eq. (5) takes the form

$$F_i(s) = F_i^*(s) \left\{ 1 \mp 2 \sum_{l'=0}^{\infty} (2l'+1) \int_{k_0}^{\infty} dp \int_0^{k_0} dq \times [ipq D_{1l'}(p, q)]^2 \int dt_1 \int dt_2 e^{i(p^2 - q^2)(t_1 - t_2)} \right\}, \quad (9)$$

where $F_i^*(s)$ is the open-line contribution. The integration domain of (t_1, t_2) is $[0 < t_1 < s$ or $0 < t_2 < s$ and $t_1 < t_2]$ in emission and $0 < t_1 < t_2 < s$ in absorption. After performing this integration and dropping the terms proportional to s , which only produce a band shift irrelevant to the present problem, Eq. (9) is substituted in (4). This gives

$$I_i(\omega) = I_i^*(\omega) + \int_{k_0}^{\infty} dp \int_0^{k_0} dq \times \{ I_i^*(\omega) - I_i^*[\omega \pm (p^2 - q^2)] \} \frac{4pq\sigma(p, q)}{(p^2 - q^2)^2}, \quad (10)$$

with

$$\sigma(p, q) = -\frac{1}{2}pq \sum_{l'=0}^{\infty} (2l'+1) [D_{l'}(p, q)]^2 . \quad (11)$$

The star still refers to the open-line contribution. At the Fermi edge, i. e., for the frequency $\omega_0 \mp \epsilon$, with $\epsilon = |\omega - \omega_0|$ vanishing, Eq. (10) can be written

$$I_1(\sim \omega_0) = I_1^*(\sim \omega_0) \left\{ 1 + \int_{k_0}^{\infty} dp \int_0^{k_0} dq \frac{4pq}{(p^2 - q^2)^2} \right. \\ \left. \times [\sigma(p, q) - \sigma(k_0, k_0)] + \sigma(k_0, k_0) \int_{k_0}^{\infty} dp \int_0^{k_0} dq \right. \\ \left. \times \frac{4pq}{(p^2 - q^2)^2} \eta(p^2 - q^2 - \epsilon) \right\} .$$

The last double integral gives $1 + \ln(\omega_0/\epsilon)$ and we obtain

$$I_1(\sim \omega_0) = I_1^*(\sim \omega_0) [1 + E_0(\epsilon)] , \quad (12)$$

with

$$E_0(\epsilon) = \sigma(k_0, k_0) [L + \ln(\omega_0/\epsilon)] \quad (13)$$

and

$$L = 1 + \int_{k_0}^{\infty} dp \int_0^{k_0} dq \frac{4pq}{(p^2 - q^2)^2} \left[\frac{\sigma(p, q)}{\sigma(k_0, k_0)} - 1 \right] . \quad (14)$$

Let us now introduce the phase shifts in the Born approximation which at the Fermi level are related to the core-hole vertex function D_i , defined in Eq. (B1), by

$$\delta_i = \frac{1}{2} \pi k_0 D_i(k_0, k_0) \\ = (8\pi k_0)^{-1} \int_0^{2k_0} dk kv(k) P_1(1 - k^2/2k_0^2) . \quad (15)$$

Then, using Eqs. (8) and (11), one has

$$\sigma_0 = \sigma(k_0, k_0) \quad (16)$$

for the negative term of the exponent α_i . Equation (12) can then be considered as the first two terms of (1) in a σ_0 expansion. Up to now, two approximations are made: (i) Only one loop is used; (ii) this loop has only two vertices, this latter approximation being equivalent to the Born approximation.

At the Fermi edge, however, the one-loop approximation can be brought back to a many-loop treatment. Indeed, in Eq. (12) I_1^* appears as a general factor, and such is the case for all the other terms related to any number of loops. Moreover, the second factor of (12), which has the form $1 + E_0$, can be continued as $1 + E_0 + \frac{1}{2}E_0^2 + \dots = e^{E_0}$, and (12) can then be restored into the power form

$$I_1(\sim \omega_0) = I_1^*(\sim \omega_0) (\xi_0/\epsilon)^{\sigma_0} , \quad (17)$$

with

$$\xi_0 = \epsilon e^{E_0(\epsilon)/\sigma_0} \\ = \omega_0 e^L . \quad (18)$$

This method is exact only at the Fermi edge but it also provides a good approximation at other fre-

quencies. Let us consider again n loops instead of 1. The new terms coming in Eq. (10) will contain convolution factors like $I_i^*(\omega \pm \sum_{i \leftarrow n} (p_i^2 - q_i^2))$ which are not too troublesome. Indeed the integrands peak strongly at $p_i^2 - q_i^2 \sim 0$, and the arguments of I_i^* can be simplified into $\omega \pm (p_i^2 - q_i^2)$, in such a way as to allow a factorization. Equation (10) can then also be generalized to any number of loops, giving the exponential form

$$I_1(\omega) = I_1^*(\omega) e^{E(\omega)} , \quad (19)$$

with

$$E(\omega) = \int_{k_0}^{\infty} dp \int_0^{k_0} dq \\ \times \left[1 - \frac{I_i^0[\omega \pm (p^2 - q^2)]}{I_i^0(\omega)} \right] \frac{4pq\sigma(p, q)}{(p^2 - q^2)^2} . \quad (20)$$

Writing $E(\omega) = \sigma_0 \ln[\xi(\omega)/|\omega - \omega_0|]$, we obtain for $\xi(\omega)$ the expression

$$\xi(\omega) = |\omega - \omega_0| e^{E(\omega)/\sigma_0} , \quad (21)$$

which tends to Eq. (18) at the Fermi edge, in the same way as (10) tends to (12).

In the framework of the Born approximation, we obtain in this way an expression for $\xi(\omega)$ for the closed-loop part. This expression is correct at the Fermi edge as given by Eqs. (18) and (14) and may be extended to other frequencies in the form (21), as long as $|\omega - \omega_0|$ does not exceed the Fermi energy.

The next point will consist in showing that the Born δ_i 's given by (15) are satisfactory at the Fermi momentum. If this is true, it implies that Eqs. (16) and (11) will yield, as a good approximation, the second term σ_0 of the exponent α_i , and that the loops with more than two vertices will only contribute a small correction to (21).

IV. BORN PHASE SHIFTS

The δ_i 's are expressed in the Born approximation by Eq. (15), where $v(k)$ represents the effective potential seen by a conduction electron. This potential takes into account the screening effect of the other conduction electrons and the structure of the core hole. These two effects are separated if we write

$$v(k) = v_{ps}(k)/\epsilon(k) , \quad (22)$$

where $v_{ps}(k)$ is a pseudopotential containing all the core structure, the conduction electrons being described by plane waves; $\epsilon(k)$ is the Lindhard static dielectric constant related to the screening effect. For small k , $v(k)$ tends to the Thomas-Fermi potential

$$v_{TF}(k) = \frac{8\pi a_B^{-1}}{k^2 + k_s^2} , \quad (23)$$

with $k_s^2 = 4k_0/\pi a_B$.

Up to now we only know the values of α_l and δ_l proposed by Ausman and Glick¹¹ for Li and Na. We shall begin by showing that these values are very close to the ones obtained by means of the Born expression (15) and the above Thomas-Fermi potential. By substitution of Eq. (23) into (B5) or (15), one has a solvable integral,¹⁵ giving

$$D_l(p, q) = \frac{2}{\pi a_B p q} Q_l \left(\frac{p^2 + q^2 + k_s^2}{2 p q} \right), \quad (24)$$

where Q_l is a Legendre polynomial of the second kind. Hence, one has

$$\delta_l = (a_B k_0)^{-1} Q_l(1 + k_s^2/2k_0^2). \quad (25)$$

Concerning α_l , let us consider $\sigma(p, q)$ given by Eq. (11) or (B6). In Appendix B, (B6) is shown to be equivalent to (B8), i. e.,

$$\sigma(p, q) = - (2\pi)^{-4} \int_{|p-q|}^{p+q} dk k [v(k)]^2, \quad (26)$$

which applies to any local pseudopotential. In the special case of the Thomas-Fermi potential and for $p = q = k_0$, Eq. (26) becomes $\sigma_0 = -\frac{1}{2}(1 + \pi a_B k_0)^{-1}$. This gives, with Eq. (25), the following very simple expressions for δ_l and α_l :

$$\delta_l = \frac{1}{2} \pi (x - 1) Q_l(x), \quad (27)$$

$$\alpha_l = (x - 1) [Q_l(x) - \frac{1}{2}(x + 1)^{-1}], \quad (28)$$

with

$$x = 1 + 2(\pi a_B k_0)^{-1} = 1 + 0.33 r_s.$$

In the case of Li ($r_s = 3.28$) and Na ($r_s = 3.96$), we obtain the values given in Table I, where they are compared with Ausman and Glick's results. The agreement is very good. But such an agreement must be explained, since at first sight the Born approximation seems rather crude, especially concerning δ_0 .

The condition of validity of the Born expression (15) is $v(r) \ll k_0^2$ at the distance $r \gtrsim [l(l+1)]^{1/2}/k_0$. Using the r -dependent Thomas-Fermi potential $v_{TF}(r) = 2(a_B r)^{-1} e^{-k_s r}$, this condition becomes

$$e^{-(4l(l+1)/\pi a_B k_0)^{1/2}} \ll \frac{1}{2} [l(l+1)]^{1/2} a_B k_0,$$

which is satisfied only for $l \geq 1$. In other words,

Eq. (15) is valid for all the δ_l 's except δ_0 . This latter δ_0 can now be calculated with the help of the Friedel sum rule, that is,

$$\delta_0 = \frac{1}{2} \pi - \sum_{l=1}^{\infty} (2l+1) \delta_l, \quad (29)$$

where the Born δ_l 's can be substituted in the second member. But this will also provide a Born δ_0 given by (15). Such a result is due to the fact that the Born phase shifts at the Fermi level satisfy exactly the Friedel sum rule. This property of the Born δ_l 's can easily be verified by means of Eqs. (15), (B4), and (B7) with $r = r'$, which give

$$\begin{aligned} \sum_{l=0}^{\infty} (2l+1) \delta_l &= k_0 \int_0^{\infty} dr r^2 v(r) \sum_{l=0}^{\infty} (2l+1) [j_l(k_0 r)]^2 \\ &= (k_0/4\pi) [v(k)]_{k=0}. \end{aligned}$$

For $k=0$, potential (23), as well as potential (22), have the limit $8\pi/a_B k_s^2 = 2\pi^2/k_0$, and this verifies the sum rule. The Born δ_l 's can now be shown to be acceptable. Indeed let $\Delta\delta_l$ be the error introduced in δ_l by the Born approximation. For $l \neq 0$, $\Delta\delta_l/\delta_l$ is small. On the other hand, δ_0 and $\frac{1}{2}\pi - \delta_0$ are of the same order, as can be seen in Table I. Hence according to Eq. (29), one has

$$\begin{aligned} \Delta\delta_0/\delta_0 &\approx \Delta\delta_0 / (\frac{1}{2}\pi - \delta_0) = \sum_{l=1}^{\infty} (2l+1) \Delta\delta_l / \sum_{l=1}^{\infty} (2l+1) \delta_l \\ &\approx \Delta\delta_l/\delta_l \quad (\text{with } l \neq 0), \end{aligned}$$

which shows that $\Delta\delta_0/\delta_0$ also is small.

The agreement with Ausman and Glick is particularly interesting because these authors use quite a different method and approximations. However, their method is not so straightforward. It consists in substituting a nonseparable potential in an expression established by ND for a separable potential. Furthermore this expression [Eq. (43) of ND] is nothing else than the solution of an equation established by Kohn¹⁶ for a very general potential, solved by ND precisely because they use the approximation of the separable potential. This introduces in Ausman and Glick's calculations a number of approximations which are hard to estimate and which finally require the introduction of a scaling parameter g to satisfy the Friedel sum rule. This parameter is taken as being of the order of

TABLE I. Phase shifts and ND exponent for Li and Na. The numbers in parentheses are those proposed by Ausman and Glick (Ref. 11).

l	Li ($r_s = 3.28$),		Na ($r_s = 3.96$),	
	δ_l	α_l	δ_l	α_l
0	0.891 (0.914)	0.391 (0.409)	0.955 (0.921; 1.04)	0.410 (0.398; 0.433)
1	0.152 (0.149)	-0.079 (-0.104)	0.145 (0.163; 0.133)	-0.106 (-0.085; -0.148)
2	0.031 (0.025)	-0.156 (-0.183)	0.026 (0.024; 0.019)	-0.181 (-0.173; -0.220)
3	0.007 (0.005)	-0.172 (-0.196)	0.005 (0.004; 0.003)	-0.195 (-0.186; -0.230)
4	0.0015 (0.0011)	-0.175 (-0.198)	0.0010 (0.0008; 0.0007)	-0.198 (-0.188; -0.232)

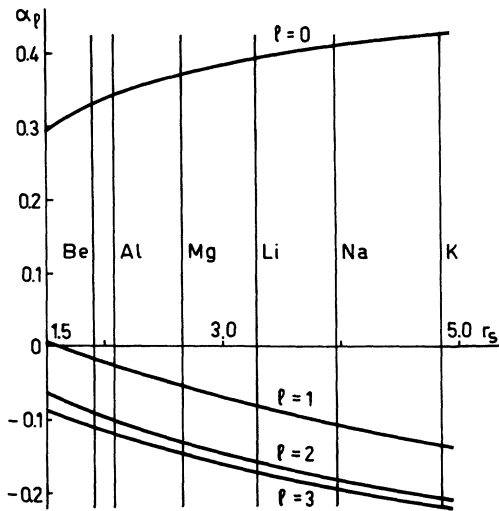


FIG. 3. Exponent α_l as a function of the electron-density parameter r_s , according to Eq. (28).

0.6, while it should normally be very close to 1; moreover it depends, although weakly, on the magnetic quantum number of the core hole, which is not to be expected on physical grounds. Our method, which is much simpler, may in a sense extend Ausman and Glick's conclusion for Li and Na to other metals, according to which conclusion α_l is positive only for $l=0$. This conclusion appears verified on Fig. 3. It should be noted that a spike in K bands ($\alpha_1 > 0$) would require $r_s \lesssim 1.6$, a density too high for the normal metals, except perhaps Be.

One may, however, wonder whether the values given by Eqs. (27) and (28), and by the way by Ausman and Glick, are not overestimated for δ_0 . Indeed those values for $l \neq 0$ are probably a bit too small, the Thomas-Fermi screen being too strong for small distances. Equation (29) would then indicate that $\delta_0 = 0.96$ given in Table I for Na is probably overestimated. On the other hand, if we use a pseudopotential, for instance the Ashcroft pseudopotential,¹⁷ we obtain a very small δ_0 . Ashcroft proposes for Na a pseudopotential having a core radius of 1.66 a.u. This radius is a cutoff distance below which the Coulomb potential is canceled by the core effect. This would give $\delta_0 = 0.53$, surely too small. However, using a comment made by Ashcroft,¹⁸ his core radius can be decreased to take account of the inner-shell ionization. The point is to know how much the core radius has to be so modified. Towards this end, one may look for a relationship between the core radius R_c proposed by Ashcroft and some atomic property like, for instance, the orbital radius of the valence electron in a free atom.¹⁹ To determine this, we can use the rather simple technique provided by the Slater rules.²⁰ In Fig. 4 we represent the core radius

proposed by Ashcroft for seven metals versus the radius R_{sl} of the Slater valence orbital in the free atom. The related points are practically located on a straight line passing through the origin, the largest deviation being $\approx 12\%$. Concerning the present problem, we have by the way a method to estimate the change in the Ashcroft radius if an electron is missing in a core shell. We compute the new orbital radius of the valence electron by means of the Slater rules and then use the linear relation emphasized on Fig. 4. For Na, one has, according to Slater rules (in atomic units),

$$R_{sl} = n^*/(Z - s) = 3/(11 - 8 \times 0.85 - 2 \times 1.00) = 1.364$$

and, if a $2p$ electron is missing,

$$R_{sl}^* = 3/(11 - 7 \times 0.85 - 2 \times 1.00) = 0.987.$$

Hence we deduce the modified core radius of Na:

$$R_c^* = R_c R_{sl}^*/R_{sl} = 1.20 \text{ a.u.}$$

instead of $R_c = 1.66$ a.u. For Li, the same method gives $R_c^* = 1.21$ a.u. for a missing $1s$ electron instead of $R_c = 2.00$ a.u.

As shown in Table II, the modified R_c^* gives values for δ_l and α_l closer to the Thomas-Fermi values, and then may be expected to be rather close to the actual values. In Sec. VI, we will use the OPW method, which is more accurate, than the previously mentioned "modified" pseudopotential method. We obtain the results given in the last row of Table II. These results are rather similar to the preceding ones. However for Li, α_1 is again negative as obtained by Ausman and Glick and as suggested by observed K bands.

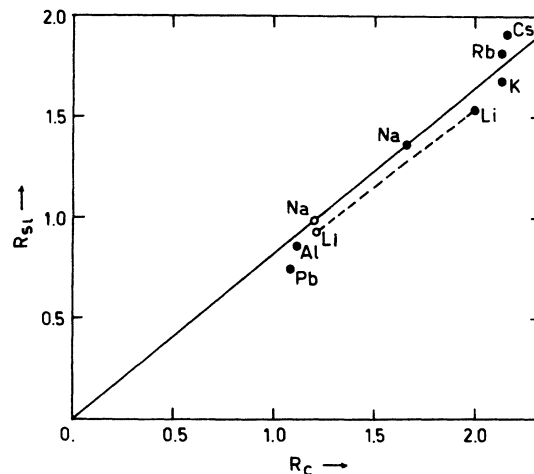


FIG. 4. Ashcroft core radius R_c vs the Slater radius R_{sl} of the valence orbital for seven metals (closed circles). If a core electron is missing, one can estimate the modified R_c (open circles) by computing the new R_{sl} and then by using the quasilinear law shown in this figure.

TABLE II. Phase shift, exponent, and constant ξ_0 of Eq. (1) calculated using (a) the Thomas-Fermi potential, the Ashcroft pseudopotential (b) with a normal core radius and (c) with a modified core radius, and (d) the OPW method of Sec. VI; ξ_0 is defined by Eqs. (18) and (14).

	Na $L_{2,3}$ band			Li K band			Be K band		
	δ_0	α_0	ξ_0	δ_1	α_1	ξ_0	δ_1	α_1	ξ_0
(a) TF	0.96	0.41	0.417	0.15	-0.079	0.401	0.15	-0.018	0.359
(b) R_c	0.53	0.24	0.333	0.29	0.122	0.390
(c) R_c^*	0.76	0.34	0.353	0.21	0.035	0.324
(d) OPW	0.70	0.33	0.349	0.14	-0.057	0.365	0.16	0.016	0.307

The use of the pseudopotential is very straightforward, but is probably not quite safe, especially if large k 's are involved in the calculations, as could be the case for the open-line contribution. In any way it gives, concerning the exponent α_i , results which are certainly a good estimation of it.

The conclusion of this section concerning the closed-loop contribution to the ND problem is that the two vertex loops give the dominant contribution. It is indeed those loops which allow us to get results similar to those of Ausman and Glick¹¹ and probably even better results, according to the way the short-range structure is treated.

V. OPEN-LINE CONTRIBUTION

The introduction of a realistic potential in the open-line part of the diagrams seems more difficult. In this case it is not possible to isolate dominating diagrams as was done in the case of the closed-loop part. At the Fermi edge, this open line is shown by ND to give a power divergence of the form

$$I_i^*(\omega) \propto (\xi_0/\epsilon)^{2\delta_i/\pi} = e^{[(2\delta_i/\pi)\ln(\xi_0/\epsilon)]}. \quad (30)$$

If we only use open lines with a finite number of vertices, it is, of course, not possible to reproduce this exponential form.

Let us consider, however, the expansion

$$I_i^*(\omega) = I_i^0(\omega) + I_i^1(\omega) + I_i^2(\omega) + \dots, \quad (31)$$

where the successive terms relate to open lines with 0, 1, 2, etc., vertices located in the unshaded regions of Fig. 2. The general form of the n vertex term is, according to the rules of Appendix C,

$$I_i^n(\omega) = \sum_{\theta_i = \pm} \sum_{\alpha \neq \theta} (\pm \pi) \int dk' \int dk_1 \int dk_2 \dots \int dk_n \int dk \\ \times [k'^{i+1} h_i(k')] \theta' [k'_1 D_i(k', k_1)] \\ \times \theta_1 [k_1 k_2 D_i(k_1, k_2)] \theta_2 \dots \\ \times \theta_{n-1} [k_{n-1} k D_i(k_{n-1}, k)] \theta [k^{i+1} h_i(k)], \quad (32)$$

where the θ 's represent $[\omega \pm k_i^2 + \sum_{p,q} (k_p^2 - k_q^2)]^{-1}$, except one of them, which is the δ function $\delta(\omega \pm k_i^2 + \sum_{p,q} (k_p^2 - k_q^2))$. The signs \pm and the k -integration

limits, $(0, k_0)$ or (k_0, ∞) , depend on the hole or particle character of the corresponding k states. The first sum goes over the $n+1$ possible choices of the δ function among the θ 's, and the second sum is over the $n!$ possible arguments of these functions.

We will make two assumptions. The first, also made in Sec. IV for the closed-loop part, is still valid for the open-line part: The phase shifts given by the Born expression (15) are satisfactory. The other assumption, which will be dropped later for the lowest-order terms, is the following: We will assume, as in ND and Ref. 14, that $D_i(k, k')$ is separable and write

$$kk' D_i(k, k') = u(k^2) u(k'^2). \quad (33)$$

Let us write for simplicity

$$k^{i+1} h_i(k) = w(k^2) \quad (34)$$

and introduce the following functions:

$$U(\omega) = \pm 2 \int dk \frac{[u(k^2)]^2}{\omega - k^2}, \quad (35)$$

$$V(\omega) = \pm 2 \int dk \frac{u(k^2) w(k^2)}{\omega - k^2}, \quad (36)$$

$$U'(\omega) = \pi \int dk [u(k^2)]^2 \delta(\omega - k^2) = \frac{1}{2} \pi \omega^{-1/2} [u(\omega)]^2, \quad (37)$$

$$V'(\omega) = \pi \int dk u(k^2) w(k^2) \delta(\omega - k^2) \\ = \frac{1}{2} \pi \omega^{-1/2} u(\omega) w(\omega), \quad (38)$$

$$W'(\omega) = \pi \int dk [w(k^2)]^2 \delta(\omega - k^2) = \frac{1}{2} \pi \omega^{-1/2} [w(\omega)]^2 \\ = I_i^0(\omega). \quad (39)$$

The signs in Eqs. (35) and (36), and the integration limits, $(0, k_0)$ or (k_0, ∞) , depend on the hole or particle character of the state k .

In addition to Eq. (33), ND also assumed that $w(k^2)$ and $u(k^2)$ were proportional functions. (We, however, will not use this assumption.) Using the Born phase shifts and this second assumption of ND, i. e., $w(k^2) = cu(k^2)$, we could write (30) in the form

$$I_i^*(\omega) = I_i^0(\omega) e^{U(\omega)}$$

$$= c^2 \sum_{n=0}^{\infty} (n!)^{-1} U'(\omega) [U(\omega)]^n, \quad (40)$$

which would mean that

$$I_l^n(\omega) = c^2 (n!)^{-1} U'(\omega) [U(\omega)]^n. \quad (41)$$

In other words, the initial and final radiative vertices of the open line would be treated on the same footing as the vertices related to the interaction with the core hole. In that case, all the free propagators contributing to the open-line part are of the same type as in the closed-loop part. This shows, by referring to Eqs. (35), (33), (15), and to the closed-loop results, that we could write

$$U(\omega) = (2\delta_l/\pi) \ln [|\xi_l(\omega)/|\omega - \omega_0|], \quad (42)$$

which is consistent with ND results as well as with the results and discussion of Secs. III and IV. Index l in ξ_l means that, in the definition (21) and (20) of ξ , $\sigma(p, q)$ and σ_0 are replaced by $\sigma_l(p, q)$ and σ_{l0} , where

$$\sigma_l(p, q) = -\frac{1}{2} p q (2l+1) [D_l(p, q)]^2, \\ \sigma_{l0} = -2(2l+1)(\delta_l/\pi)^2.$$

The situation, however, is not so simple if we consider $w(k^2)$ and $u(k^2)$ as being two different functions. In this more realistic situation, the second member of Eq. (41) has also to contain $V(\omega)$ and $V'(\omega)$. To see how to modify (41), let us consider (32). The first summation in Eq. (32) is carried over $n+1$ terms. Two of these terms are obtained by substituting a δ function for θ or θ' , which means that in (41) $U'U^n$ has to be replaced by $V'U^{n-1}V$. The $n-1$ other terms of Eq. (32) are obtained by the substitution of a δ function for one of the $\theta_1, \dots, \theta_{n-1}$ which in (41) would modify $U'U^n$ into $VU'U^{n-2}V$. All that shows that Eq. (41) has to be replaced for $n \geq 2$ by

$$I_l^n = [(n+1)!]^{-1} [2V'U^{n-1}V + (n-1)VU'U^{n-2}V]. \quad (43)$$

For $n=1$, one simply has $I_l^1 = V'V$ and, for $n=0$, $I_l^0 = W'$. These I_l^n can now be added to obtain the exponential form. One gets

$$I_l^*(\omega) = I_l^0(\omega) [A(\omega)e^{U(\omega)} + B(\omega)], \quad (44)$$

with

$$A = C^2 + 2C(1-C)U^{-1}, \quad (45)$$

$$B = (1-C)(1-C-2CU^{-1}), \quad (46)$$

and

$$C = \frac{uV}{wU}, \quad (47)$$

where A , B , C , U , V , u , and w depend on ω . The U and V expansion of Eq. (44) is thus equivalent to (31), the successive terms being

$$I_l^0(\omega) = \frac{1}{2} \pi \omega^{1+1/2} [\hbar(\omega^{1/2})]^2, \quad (48)$$

$$I_l^1(\omega) = I_l^0(\omega) C(\omega) U(\omega), \quad (49)$$

$$I_l^n(\omega) = [I_l^0(\omega)/(n+1)!] [2 + (n-1)C(\omega)] \\ \times C(\omega) [U(\omega)]^n \text{ for } n \geq 2. \quad (50)$$

It is interesting to note that $I_l^1(\omega)$, as well as $I_l^0(\omega)$, is not affected by the separability assumption (33). Indeed for $n=1$, Eq. (32) becomes

$$I_l^1(\omega) = -2 \int_0^\infty dk' \eta(\pm k_0 \mp k') \int_{k_0}^\infty dk \\ \times k'^{1+2} \hbar_l(k') \pi \delta(\omega - k'^2) \\ \times D_l(k', k) (\omega - k^2)^{-1} k^{1+2} \hbar_l(k), \quad (51)$$

where the separability is not required to perform the integration. One obtains (49) with

$$C(\omega) U(\omega) = 2 \int_{k_0}^\infty dk \frac{k^2}{k^2 - \omega} \\ \times \left(\frac{k}{\omega^{1/2}} \right)^l \frac{\hbar_l(k)}{\hbar_l(\omega^{1/2})} D_l(k, \omega^{1/2}). \quad (52)$$

For $n=3$, the agreement between Eqs. (50) and (32) is no more exact, but still very good, especially concerning the dominant term, where $\theta_1(\omega - k_1) = \delta(\omega - k_1)$. Equation (44), where U is given by (42) and CU by (52), thus restores the lowest-order terms without requiring the separability of $D_l(k, k')$. Concerning the higher-order terms, a result of the same type as the closed-loop contribution can be obtained using the same $\xi(\omega)$.

Grouping Eqs. (19) and (44), we obtain Eq. (3) with

$$G(\omega) = A(\omega) [\xi_l(\omega)/\xi(\omega)]^{2\theta_l/\pi} \\ + B(\omega) [|\omega - \omega_0|/\xi(\omega)]^{2\theta_l/\pi}. \quad (53)$$

This gives an expression of the edge behavior of band spectra which is not only a good approximation of the ND result regarding the exponent value, but which also describes the absolute intensity of the bands, in the frequency range of about ω_0 above (or below) this edge, in emission (or absorption). An important point has to be emphasized, which is the singularity in the slope of $G(\omega)$, right at the Fermi edge. This point, not mentioned until now, will be discussed in Sec. VII. However, before surveying the present results, we would like to present more detailed calculations where the pseudopotential method, used up to now, namely, in the expression of $D_l(p, q)$, is finally replaced by the more elaborate OPW method.

VI. INTRODUCTION OF THE OPW'S

In this section some details are given about the calculation of $\xi(\omega)$ and $G(\omega)$. The following two cases are considered: (i) The conduction electrons are described by plane waves (PW) and the inter-

action $v(k)$ with the core hole is represented by a pseudopotential. (ii) The electrons are described by OPW's and $v(k)$ represents the screened Coulomb potential of the core hole. This latter approach is better, since the pseudopotential is not fitted for large k 's whose contribution may be important, particularly in the open-line part, as was shown previously.¹⁰

The difference between the two approaches essentially appears in the treatment of $D_i(p, q)$, as given by Eq. (B1). In the first method, the function $u_i(k, r)$ appearing in (B1) is the Bessel function $j_l(kr)$, and $v(k)$ is given by Eq. (22), where we use the Ashcroft pseudopotential¹⁷ $v_{ps}(k) = 8\pi(a_B k^2)^{-1} \cos(kR_c)$. In the second method the more sophisticated $u_i(k, r)$ given by (A3) is used and the potential is

$$v(k) = g(k) v_{cb}(k) / \epsilon(k), \quad (54)$$

where $v_{cb}(k) = 8\pi(a_B k^2)^{-1}$ is the Coulomb potential and $g(k)$ is the charge density of the core hole. In coordinate space, Eq. (54) has the form

$$v(r) = \int d\vec{x}' |\psi_c(\vec{x}')|^2 v^*(|\vec{x}' - \vec{x}|),$$

where $v^*(r)$ is the Fourier transform of $v_{cb}(k)/\epsilon(k)$. This shows that $g(k)$ is given by $g(k) = \langle \psi_c | e^{i\vec{k}\cdot\vec{r}} | \psi_c \rangle$. If ψ_c is degenerate, an average is performed over the degenerate states to take account of the flipping due to the electron collisions. Explicit expressions of $g(k)$ are given in Appendix A, namely, Eq. (A13) for the Na $L_{2,3}$ state and Eq. (A14) for the K state in Li or Be.

The expression of $\xi(\omega)$ essentially appears in the close-loop calculation of Eq. (21), where (20) and (11) are used.

In the PW case, where $\sigma(p, q)$ is given by (26), it is easier to change the order of integrations. One obtains

$$E(\omega) = - (2\pi)^{-4} \int_0^\infty dk k [v(k)]^2 \int_0^\infty d\omega' \omega'^{-2} \times [1 - I_l^0(\omega \pm \omega') / I_l^0(\omega)] T(k, \omega'), \quad (55)$$

with $\omega' = p^2 - q^2$ and

$$T(k, \omega) = \begin{cases} \omega' & \text{for } 0 < \omega' < k - k^2 \\ \frac{1}{4} [1 - (\omega' / k - k)^2] & \text{for } |k - k^2| < \omega' < k + k^2 \\ 0 & \text{elsewhere} \end{cases}$$

Incidentally we notice that $T(k, \omega)$ is directly related to the Lindhard dynamical dielectric constant by the relation $v_{cb}(k) T(k, \omega) = 8\pi k \text{Im} \epsilon(k, \omega)$. Such a relation is not surprising since the Lindhard $\epsilon(k, \omega)$ is also calculated in the two-vertex-loop approximation. The ω' integration can then be performed analytically in (55) if $I_l^0(\omega) = \frac{1}{2}\pi\omega^{l+1/2} [h(\omega^{1/2})]^2$ is approximated by $I_l^0(\omega) \approx \frac{1}{2}\pi\omega^{l+1/2} [h(0)]^2$. This as-

sumption considerably simplifies the calculations and introduces only a small change in Eq. (55), since the integrand peaks strongly for $\omega' \approx 0$. So only a simple integral over k remains, which can be performed numerically. At the Fermi frequency the divergent term has to be extracted first, as in Eq. (13). Then L , given by Eq. (14), can be computed in the same way as $E(\omega)$.

Once $\xi(\omega)$ and $\xi_l(\omega)$ are known, one can calculate $G(\omega)$ given by (53). In Eq. (53), $A(\omega)$ and $B(\omega)$ are given by (45) and (46), using $C(\omega)$ and $U(\omega)$ defined by (52) and (42). So the main problem is to calculate $C(\omega)U(\omega) = I_l^1(\omega)/I_l^0(\omega)$ as given by (52), the rest of the calculation being straightforward.

First let us consider again the PW case. Using Eq. (B5) and changing the order of integrations, (52) becomes

$$C(\omega)U(\omega) = (2\pi^2)^{-1} \int_0^\infty dk k v(k) M_l(k, \omega) \quad (56)$$

with, by writing $\omega \equiv u^2$,

$$M_l(k, u^2) = \eta(k - k_0 + u) \int_{\max(k_0, |k-u|)}^{k+u} dp (p^2 - u^2)^{-1} \times \left(\frac{p}{u}\right)^{l+1} \frac{h_l(p)}{h_l(u)} P_l\left(\frac{p^2 + u^2 - k^2}{2pu}\right). \quad (57)$$

The integration in this expression can be performed analytically. Let us note that, here, replacing $h_l(p)$ and $h_l(u)$ by $h_l(0)$ could introduce a serious error since the large p 's play an important role, especially when $l \geq 1$. Anyway, the analytic integration of Eq. (57) is possible here, even with the exact $h_l(p)$. For the Fermi frequency $\omega = \omega_0$, i. e., $u^2 = k_0^2$, the divergent term has also to be isolated in (57), by writing

$$M_l(k, \sim \omega_0) = \eta(2k_0 - k)(2k_0)^{-1} P_l(1 - k^2/2k_0^2) \ln(\omega_0/\epsilon) + \text{convergent terms.} \quad (58)$$

This divergent term substituted in Eq. (56) gives, using (B5) and (B3),

$$C(\sim \omega_0)U(\sim \omega_0) = (2\delta_l/\pi) \ln(\omega_0/\epsilon) + \text{convergent terms.}$$

Looking now at Eq. (42), one sees that $C(\omega_0) = 1$; thus $G(\omega_0) = [\xi_l(\omega_0)/\xi(\omega_0)]^{2\delta_l/\pi}$ is finite at the Fermi edge (an practically equal to 1). However, special attention must be paid to $G(\omega)$ in the Fermi-edge region, where it varies rapidly, as shown on Fig. 7. In that region, using expressions like (58) and (59), where the diverging term is explicitly written, may considerably increase the precision of the numerical calculations.

Until now, we have only considered the PW treatment, which is the first step in the OPW method. The introduction of the OPW's requires first the use of Eq. (54) instead of the pseudopotential,

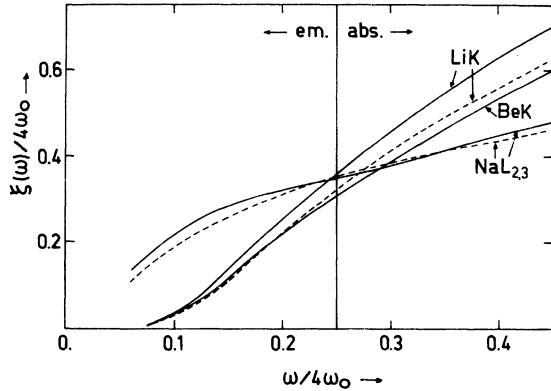


FIG. 5. Frequency dependence of $\xi(\omega)$ using the pseudopotential method (dashed curves) and the OPW method (solid curves).

then the introduction of additional terms in $E(\omega)$, for the $\xi(\omega)$ calculation, and in $C(\omega)U(\omega)$, for the $G(\omega)$ calculation. According to Eqs. (20) and (B11) on one hand, and according to Eqs. (52) and (B9) on the other, those terms are, respectively,

$$\Delta E(\omega) = \int_{k_0}^{\infty} dp \int_0^{k_0} dq \times \left[1 - \frac{I_1^0[\omega \pm (p^2 - q^2)]}{I_1^0(\omega)} \right] \frac{4pq\sigma^c(p, q)}{(p^2 - q^2)^2}$$

and

$$\Delta[C(\omega)U(\omega)] = 2 \int_{k_0}^{\infty} dk \frac{k^2}{k^2 - \omega} \times \left(\frac{k}{\omega^{1/2}} \right)^i \frac{h_i(k)}{h_i(\omega^{1/2})} D_i^c(k, \omega^{1/2}),$$

where $\sigma^c(p, q)$ and $D_i^c(p, q)$ are given in Appendix B. Here the calculations are mainly numerical, the first step being the tabulation of σ^c and D_i^c . Let us note, however, that for the K bands of Li and Be, one has $\Delta[C(\omega)U(\omega)] = 0$, since $D_i^c = 0$.

VII. RESULTS AND DISCUSSION

The aim of this paper is to calculate the functions appearing in Eq. (3) in a frequency range of a few electron volts, in the Fermi-edge region. In emission, our results concern almost all of the band except, however, the tailing region. The calculations are applied to three simple metals, Li, Be, and Na, where the effects due to the band structure are particularly weak and where the OPW method can be used rather easily.

The function $\xi(\omega)$ was first investigated. This function appears as a constant in ND calculations and is presented as being of the order of the Fermi energy ω_0 . This prediction is good. In Fig. 5, $\xi(\omega)/4\omega_0$ is plotted for the three metals considered and $\xi_0/4\omega_0$ values lie between 0.3 and

0.35. On the other hand, the results calculated by using a pseudopotential (dotted curves) are close to those calculated by the more precise OPW method. The value of ξ_0 can thus be estimated rather easily by means of Eqs. (18) and (14) for metals where a pseudopotential is known. Moreover Table II shows that the parameters appearing in the pseudopotential can be approximately estimated without important changes in the value of ξ_0 . In our calculations, for instance, the Ashcroft radius R_c was replaced by R_c^* , to take account of the deep core ionization, but R_c gives also a rather reliable ξ_0 . All that is due to the fact that the large k 's for which the pseudopotentials are not fitted do not play an important role in Eq. (55). The same can be said about the calculation of α_i , where an expression like (28) can easily be used for a first estimation. Concerning the ω dependence, $\xi(\omega)$ appears as an increasing but smooth function and this enables one, in a first approach, to replace $\xi(\omega)$ by a constant ξ_0 without modifying too much the edge shape. Indeed, for $L_{2,3}$ bands, where the effect of the singularity appears in a rather extended region (1 or 2 eV), the variation of $\xi(\omega)$ is particularly weak. For the K bands, however, the slope of $\xi(\omega)$ is more important, but here also $\xi(\omega)$ can be replaced by ξ_0 , since the singularity effect appears in a much smaller region, because of the small value of α_1 .

Concerning $G(\omega)$, given in Fig. 6, the situation is quite different. First, one has to take account of the detailed core structure, since here the large k 's are important. Figure 6 shows that the discrepancy between the pseudopotential results and the OPW results is large and only the latter results are reliable. Another point is that $G(\omega)$ acts as a constant in an important part of the bands. For the three metals, the constant part of $G(\omega)$

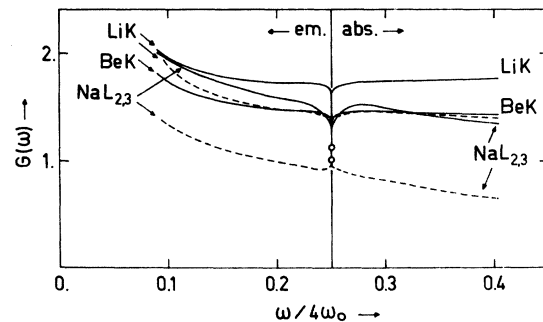


FIG. 6. Frequency dependence of $G(\omega)$ using the pseudopotential method (dashed curves) and the OPW method (solid curves). Only the OPW results are reliable. For $\omega = \omega_0$, $G(\omega_0)$ is equal to 1.03 for Na, 1.14 for Li, and 1.13 for Li. These values are represented by the open circles.

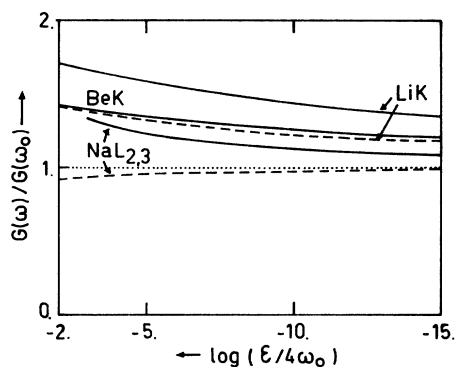


FIG. 7. Frequency dependence of $G(\omega)$ in the Fermi-edge region, using a logarithmic scale. One has $G(\omega) = G(\omega_0)$ when $\epsilon \equiv |\omega - \omega_0| = 0$, i. e., when $\ln(\epsilon/4\omega_0)$ tends to infinity.

lies between 1.5 and 1.8. At the Fermi edge, however, $G(\omega)$ presents a sudden drop and becomes practically equal to 1 (1.03 for Na, 1.14 for Li, and 1.13 for Be). These values are reached in a small frequency range, as emphasized in Fig. 7. Here we meet a new feature, not mentioned until now, since in the previous calculations the functions $u(k^2)$ and $w(k^2)$ of Eqs. (33) and (34) are supposed to be proportional. Actually, these two functions are quite different and this involves a singularity at $\omega = \omega_0$ in the slope of $G(\omega)$. This can be seen by using the expression (47) of $C(\omega)$ appearing in $G(\omega)$. When the integrals (35) and (36) are performed, $C(\omega)$ takes the form

$$C(\sim \omega_0) = \ln(K/\epsilon) / \ln(\xi_{10}/\epsilon)$$

in the Fermi-edge region, with $\xi_{10} \equiv \xi_1(\omega_0)$. For $\epsilon = 0$, one has $C(\omega_0) = 1$, which gives a finite value to $G(\omega_0)$. However, one also has $[dC/d\epsilon]_{\epsilon=0} = \infty$, except if $K = \xi_{10}$, as in the ND approximation. The slopes of $C(\omega)$ and of $G(\omega)$, at the Fermi edge, are thus completely related to the relative values of K and ξ_{10} , being infinite if $K \neq \xi_{10}$ or zero if $K = \xi_{10}$. But this latter case can appear only as an approximation, if $u(\omega) = cw(\omega)$ for instance, as supposed in ND. Actually $\ln(\xi_{10}/4\omega_0)$ and $\ln(K/4\omega_0)$ have quite different values for the metals considered. Using the OPW's, one finds $\ln(\xi_{10}/4\omega_0)$ equal to -0.99 for Na, 0.48 for Li, and 0.012 for Li; on the other hand, $\ln(K/4\omega_0)$ is equal to 0.35 for Na, 6.9 for Li, and 3.3 for Be. From these values the behavior of $G(\omega)$ is determined for $\omega \approx \omega_0$, as shown in Figs. 6 and 7.

This shows that ND expression (1), exact for $\omega \sim \omega_0$, does not completely describe the Fermi-edge structure. The function $G(\omega)$ also plays a role, especially in the K bands, where there is no Fermi-edge divergence but only a rounding off effect.

Finally, Fig. 8 gives the band shapes in emission and absorption, for Na, Li, and Be, in the frequency region where our theory is applicable. We plot $I_i^0(\omega)$ as a reference band shape, since this one-electron intensity is well known. We also

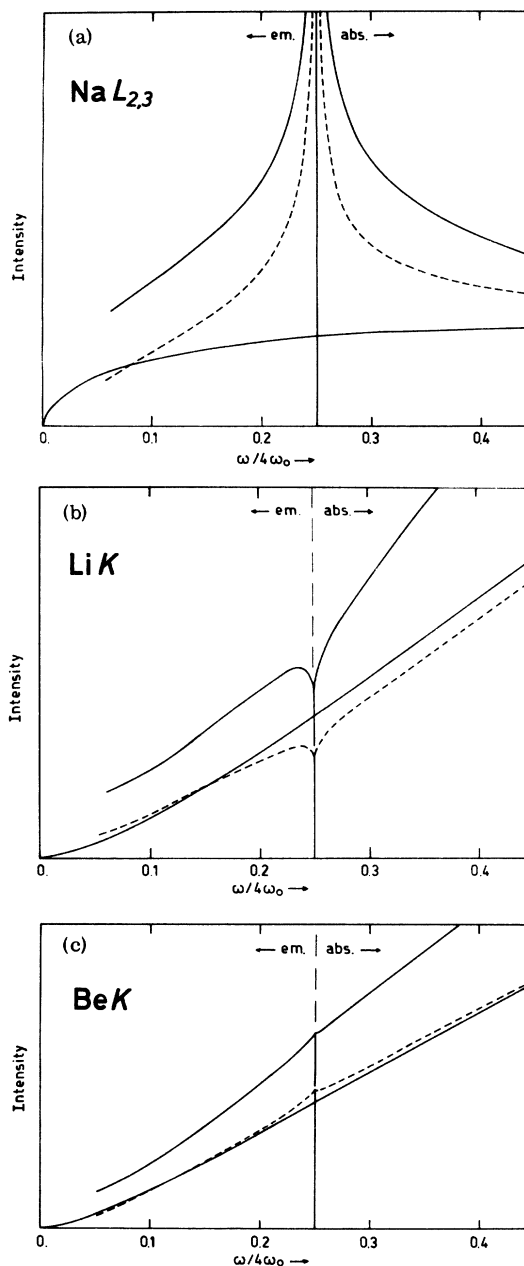


FIG. 8. Band shapes in emission and absorption (a) for $\text{Na}L_{2,3}$, (b) for $\text{Li}K$, and (c) for $\text{Be}K$. The lower solid curves are the one-electron band shapes given as a reference, especially if an absolute estimation is wanted. The upper solid curves represent $I_i(\omega)$ as given by Eq. (3), where $\xi(\omega)$ and $G(\omega)$ are calculated by the OPW method. This intensity is also given if $G(\omega)$ is supposed to be constant and equal to $G(\omega_0)$ (dashed curves).

give the band shape (dotted line), if one supposes $G(\omega) = G(\omega_0)$. The change in the band edge due to $G(\omega)$ is more evident in K bands, where the round-off effect is increased.

An important fact has still to be emphasized. Figures 8(b) and 8(c) show that the edge singularity is not sufficiently strong to explain the premature peak observed in the emission K bands of Li and Be. This could already be surmised by a look at the small values of α_1 in Table II or even in Fig. 3. (For Be, α_1 is even slightly positive.) The introduction of the singularity in the slope of $G(\omega)$ does not modify this situation very much. So it seems that an important credit has to be given back to Allotey's theory,¹³ where these premature peaks are explained by an electron-hole p -scattering resonance.

ACKNOWLEDGMENTS

The author is grateful to Professor A. J. Glick and Dr. G. A. Ausman for useful discussions, especially concerning Sec. IV. He is also thankful to Dr. K. K. Bajaj for his critical reading of the manuscript and for several useful comments. Computer facilities were afforded by the University of Liège.

APPENDIX A: WAVE FUNCTIONS AND OTHER RELATED EXPRESSIONS

We consider the core wave functions $\psi_c(\vec{x})$ as strongly localized and we describe the conduction electrons by the single OPW's:

$$\psi_{\vec{k}}(\vec{x}) = (2\pi)^{-3/2} \left[e^{i\vec{k}\cdot\vec{x}} - \sum_c \psi_c^*(\vec{k}) \psi_c(\vec{x}) \right], \quad (\text{A1})$$

where $\psi_c(\vec{k})$ is the Fourier transform of $\psi_c(\vec{x})$. As discussed in a previous paper,⁸ the OPW character of the conduction-electron wave function is important only close to the ion involved in the x-ray process. We can then write $\psi_c(\vec{x}) = R_{nl}(r) Y_l^m(\hat{x})$ and express Eq. (A1) as a sum of partial waves, that is,

$$\psi_{\vec{k}}(\vec{x}) = (2\pi)^{-3/2} 4\pi \sum_{l=0}^{\infty} \sum_{m=-l}^l i^l u_l(k, r) \bar{Y}_l^m(\vec{k}) Y_l^m(\vec{x}), \quad (\text{A2})$$

with

$$u_l(k, r) = j_l(kr) + g_l(k, r) \quad (\text{A3})$$

and

$$g_l(k, r) = - \sum_{n=1}^{l_c+1} R_{nl}(r) \int_0^{\infty} dr' r'^2 j_l(kr') R_{nl}(r'). \quad (\text{A4})$$

The functions g_l are different from zero only for $l \leq l_c$, where l_c is the largest angular momentum appearing in the core states.

We use the core-state wave functions provided by the Slater rules,²⁰ which are quite satisfactory for the metals considered in this paper, i. e.,

Na, Li, and Be. For Na, one has

$$\begin{aligned} R_{10}(r) &= 2\alpha^{3/2} e^{-\alpha r}, \\ R_{20}(r) &= 2\beta^{5/2} A [r e^{-\beta r} - 24\alpha^3 (\alpha + \beta)^{-4} e^{-\alpha r}], \\ R_{21}(r) &= 2(\beta^5/3)^{1/2} r e^{-\beta r}, \end{aligned} \quad (\text{A5})$$

with

$$A = [3 - 576 \alpha^3 \beta^5 (\alpha + \beta)^{-8}]^{-1/2},$$

and, in a. u., $\alpha = 11 - 0.30 = 10.7$ and $\beta = \frac{1}{2}(11 - 0.35 \times 7 - 0.85 \times 2) = 3.425$. Since $l_c = 1$, this gives the two functions

$$\begin{aligned} g_0(k, r) &= a(k) e^{-\alpha r} + b(k) r e^{-\beta r}, \\ g_1(k, r) &= c(k) r e^{-\beta r}, \end{aligned} \quad (\text{A6})$$

with

$$\begin{aligned} a(k) &= -8\alpha^3 [\alpha(k^2 + \alpha^2)^{-2} + 3b(k)(\alpha + \beta)^{-4}], \\ b(k) &= 8A^2 \beta^5 [(k^2 - 3\beta^2)(k^2 + \beta^2)^{-3} \\ &\quad + 24\alpha^4 (\alpha + \beta)^{-4} (k^2 + \alpha^2)^{-2}], \\ c(k) &= -\frac{32}{3} \beta^6 k (k^2 + \beta^2)^{-3}. \end{aligned}$$

For Li and Be, the only core wave function is

$$R_{10}(r) = 2\alpha^{3/2} e^{-\alpha r}, \quad (\text{A7})$$

with $\alpha = 2 - 0.30 = 1.7$ for Li and $\alpha = 3 - 0.30 = 2.7$ for Be. This gives

$$g_0(k, r) = -8\alpha^4 (k^2 + \alpha^2)^{-2} e^{-\alpha r}. \quad (\text{A8})$$

Let us now consider the x-ray transitions matrix $\langle \psi_c | \hat{n} \cdot \vec{p} | \psi_{\vec{k}} \rangle$. For the $L_{2,3}$ band of Na the transition involves the $2p$ core state. Using Eqs. (A5) and (A6), one obtains

$$\begin{aligned} \langle \psi_c | \hat{n} \cdot \vec{p} | \psi_{\vec{k}} \rangle &= 8(2\beta^7)^{1/2} (i\pi)^{-1} \\ &\quad \times [\delta_{nc} H(k) + (\frac{1}{3} \delta_{nc} k^2 - k_n k_c) (k^2 + \beta^2)^{-3}], \end{aligned} \quad (\text{A9})$$

with

$$H(k) = \left(\frac{\alpha}{\alpha + \beta} \right)^4 \frac{2\alpha - \beta Q}{\beta(k^2 + \alpha^2)^2} - \frac{Q(k^2 - 3\beta^2) + 8k^2}{24(k^2 + \beta^2)^3} \quad (\text{A10})$$

and

$$Q = \left[1 - \frac{3}{2} \left(\frac{4\alpha\beta}{(\alpha + \beta)^2} \right)^4 \right] \left[1 - \frac{3\beta}{4\alpha} \left(\frac{4\alpha\beta}{(\alpha + \beta)^2} \right)^4 \right]^{-1}.$$

The two terms in the brackets of Eq. (A9) are, respectively, related to transitions involving the s term and the d term of $\psi_{\vec{k}}$. The Kronecker δ_{nc} means that the photon polarization vector \hat{n} has the direction of the p -state ψ_c . Since, for k 's of the order of k_0 , the d term is quite negligible in (A9), Eq. (6) can be written as $W_{00}(\vec{k}) = h_0(k) Y_0^0(\hat{k})$, with

$$h_0(k) = H(k)/H(0). \quad (\text{A11})$$

The corresponding expressions are simpler for the K bands of Li and Be. According to Eqs. (A7) and

(A8), one has

$$\langle \psi_c | \hat{n} \cdot \vec{p} | \psi_{\vec{k}} \rangle = 2(2\alpha^5)^{1/2} \pi^{-1} k_n (k^2 + \alpha^2)^{-2},$$

where ψ_c is the 1s core state, so that Eq. (6) becomes $W_{1m}(\vec{k}) = kh_1(k) Y_1^m(\hat{k})$, with

$$h_1(k) = (1 + k^2/4\alpha^2)^{-2}, \quad (\text{A12})$$

where $Y_1^m(\hat{k})$ gives the photon polarization. In Eqs. (A11) and (A12) we write $h_i(k)$ in such a way as to have $h_i(0) = 1$.

Finally let us mention the expression of $g(k) = \langle \psi_c | e^{i\vec{k} \cdot \vec{x}} | \psi_c \rangle$ appearing in (54). In the case of the $L_{2,3}$ band of Na, a flipping of the $2p$ state is possible and one has, in principle, to introduce the nondiagonal matrix element

$$g_{cc'}(\vec{k}) = \langle \psi_c | e^{i\vec{k} \cdot \vec{x}} | \psi_{c'} \rangle \\ = [\delta_{cc'} - 6k_c k_{c'} (k^2 + 4\beta^2)^{-1}] (1 + k^2/4\beta^2)^{-3}.$$

However, after averaging, one has

$$g(k) = \frac{1}{3} \sum_c g_{cc}(k) \\ = (1 - k^2/4\beta^2)(1 + k^2/4\beta^2)^{-4}. \quad (\text{A13})$$

For the K bands of Li and Be, ψ_c is the nondegenerate 1s state and one has

$$g(k) = (1 + k^2/4\alpha^2)^{-2}. \quad (\text{A14})$$

APPENDIX B: FUNCTIONS $D_l(p, q)$ AND $\sigma(p, q)$

The core-hole scattering is described by the matrix element $\int d\vec{x} \vec{\psi}_p^*(\vec{x}) v(r) \psi_q(\vec{x})$, which using (A2) takes the form

$$\sum_{i=0}^{\infty} \sum_{m=-i}^i Y_i^m(\hat{p}) \bar{Y}_i^m(\hat{q}) D_i(p, q)$$

with the "core-hole-vertex" factor

$$D_i(p, q) = 2\pi^{-1} \int_0^{\infty} dr r^2 u_i(p, r) u_i(q, r) v(r). \quad (\text{B1})$$

In the two-vertex loops, Eq. (B1) contributes through a factor

$$\sigma(p, q) = -\frac{1}{2} pq \sum_{i=0}^{\infty} (2l+1) [D_i(p, q)]^2. \quad (\text{B2})$$

In this appendix, we shall give some expressions related to the two functions $D_i(p, q)$ and $\sigma(p, q)$. First let us note that for $p=q$, $D_i(p, q)$ is related to the Born-approximation phase shift. In this paper we only use the phase shift at the Fermi level and we write

$$\delta_i = \frac{1}{2} \pi k_0 D_i(k_0, k_0). \quad (\text{B3})$$

If $\psi_{\vec{x}}(\vec{x})$ is a plane wave, in other words if in Eq. (A2) $u_i(p, r) = j_i(kr)$, Eqs. (B1) and (B2) can easily be expressed as an integral in k space, where the effective potential $v(k)$ is generally known explicitly. Substituting

$$v(r) = (2\pi^2 r)^{-1} \int_0^{\infty} dk kv(k) \sin kr$$

in

$$D_i^0(p, q) = 2\pi^{-1} \int_0^{\infty} dr r^2 j_i(pr) j_i(qr) v(r), \quad (\text{B4})$$

one obtains

$$D_i^0(p, q) = (4\pi^2 pq)^{-1} \int_{|p-q|}^{p+q} dk kv(k) P_i\left(\frac{p^2 + q^2 - k^2}{2pq}\right) \quad (\text{B5})$$

or, after an evident change of variable,

$$D_i^0(p, q) = (4\pi^2)^{-1} \int_{-1}^{+1} du v[(p^2 + q^2 - 2pqu)^{-1/2}] P_i(u),$$

which can easily be computed and tabulated. To handle

$$\sigma^0(p, q) = -\frac{1}{2} pq \sum_{i=0}^{\infty} (2l+1) [D_i^0(p, q)]^2 \quad (\text{B6})$$

we use the expression²¹

$$(pR)^{-1} \sin pR = \sum_{i=0}^{\infty} (2l+1) j_i(pr) j_i(pr') P_i(u) \quad (\text{B7})$$

with $R = |\vec{x} - \vec{x}'|$ and $u = \cos(\hat{x} \cdot \hat{x}')$. Substituting (B4) in (B6), one obtains

$$\sigma^0(p, q) = -2\pi^{-2} pq \sum_{i, i'} \delta_{i, i'} (2l' + 1) \\ \times \left[\int_0^{\infty} dr r^2 j_i(pr) j_{i'}(qr) v(r) \right]^2.$$

Then replacing $\delta_{i, i'}$ by $\frac{1}{2}(2l+1) \int_{-1}^{+1} du P_i(u) P_{i'}(u)$ and using (B7) one has

$$\sigma^0(p, q) = -\pi^{-2} \int_0^{\infty} dr rv(r) \int_0^{\infty} dr' r' v(r') \\ \times \int_{|r-r'|}^{r+r'} dR R^{-1} \sin pR \sin qR.$$

The rest of the calculation is straightforward and gives

$$\sigma^0(p, q) = -(2\pi)^{-4} \int_{|p-q|}^{p+q} dk k [v(k)]^2 \quad (\text{B8})$$

which, compared to Eq. (B6), is very easy to compute.

If now $\psi_{\vec{x}}(\vec{x})$ represents the OPW (A2), one can write

$$D_i(p, q) = D_i^0(p, q) + D_i^c(p, q), \quad (\text{B9})$$

with

$$D_i^c(p, q) = 2\pi^{-1} \int_0^{\infty} dr r^2 G_i(p, q; r) v(r)$$

and

$$G_i(p, q; r) = j_i(pr) g_i(q, r) + g_i(p, r) j_i(qr) \\ + g_i(p, r) g_i(q, r).$$

Introducing again $v(k)$, one has

$$D_i^c(p, q) = \pi^{-3} \int_0^\infty dk kv(k) \left[\int_0^\infty dr r \sin kr G_i(p, q; r) \right]. \quad (\text{B10})$$

The integral in the square brackets can be performed analytically and $D_i^c(p, q)$ can then be tabulated like (B5) after computing a single integration over k . A similar treatment is applied to $\sigma(p, q)$. We write

$$\sigma(p, q) = \sigma^0(p, q) + \sigma^c(p, q) \quad (\text{B11})$$

with

$$\sigma^c(p, q) = -\frac{1}{2} pq \sum_{l=0}^{l_c} (2l+1) D_i^c(p, q) \times [D_i^c(p, q) + 2D_i^0(p, q)], \quad (\text{B12})$$

where we have only to substitute Eqs. (B5) and (B10). The advantage of Eqs. (B8) and (B12) over (B2) is twofold: $v(k)$ is used instead of $v(r)$ and the summation over an infinite number of terms does not appear any more.

APPENDIX C: DIAGRAMMATIC RULES

The diagrammatic rules are related to the cal-

ulation of $F_i(s)$ given by (5) and depend on $M_{kk'}(s)$, which is described by the diagrams of Fig. 2.

These diagrams contain two types of vertices: the radiative vertices, represented by open circles, and the vertices related to the interaction with the core hole. These core-hole vertices are essentially located on the thick lines (unshaded region of Fig. 2). The rules are the following: (i) A line, joining two vertices of any kind acting at times t_2 and t_1 , contributes through a factor

$$[\eta(k-k_0)\eta(t_2-t_1) - \eta(k_0-k)\eta(t_1-t_2)] e^{-ik^2(t_2-t_1)}.$$

The η 's are the step functions $\eta(x) = 0$ for $x < 0$ and $\eta(x) = 1$ for $x > 0$. (ii) A core-hole vertex contributes a factor $ikk'D_i(k, k')$. The function D_i is given by Eq. (B1). (iii) A radiative vertex contributes a factor $k^{l+1}h(k)$ related to the dipole matrix element by Eq. (6). (iv) Every closed-loop contribution is multiplied by a factor $-2l(l+1)$. The sum over the l 's is performed afterwards. (v) One integrates over all the k 's from 0 to ∞ and over the times (except s) from $-\infty$ to 0, and from s to ∞ in emission, or from 0 to s in absorption.

*Chercheur de l'Institut Interuniversitaire des Sciences Nucléaires Belgium.

¹P. Nozières and C. T. deDominicis, Phys. Rev. **178**, 1097 (1969).

²G. D. Mahan, Phys. Rev. **163**, 612 (1967).

³L. Hedin, in *X-Ray Spectroscopy*, edited by L. V. Azaroff (McGraw-Hill, New York, to be published), Chap. 5.

⁴R. A. Ferrell, Phys. Rev. **186**, 399 (1969).

⁵B. Bergersen, F. Brouers, and P. Longe, J. Phys. F **1**, 945 (1971).

⁶B. Bergersen, T. McMullen, and J. P. Carbotte, Can. J. Phys. **49**, 3155 (1971).

⁷G. Yuval, Phys. Rev. B **4**, 4315 (1971).

⁸P. Longe and A. J. Glick, Phys. Rev. **177**, 526 (1969).

⁹H. W. B. Skinner, Philos. Trans. R. Soc. Lond. A **239**, 95 (1940); H. Jones, N. F. Mott, and H. W. B. Skinner, Phys. Rev. **45**, 379 (1934).

¹⁰F. Brouers, P. Longe, and B. Bergersen, Solid State Commun.

8, 1423 (1970).

¹¹G. A. Ausman and A. J. Glick, Phys. Rev. **183**, 687 (1969).

¹²N. Kerr Del Grande and A. J. Oliver (unpublished).

¹³F. K. Allotey, Phys. Rev. **157**, 467 (1967).

¹⁴K. D. Schotte and U. Schotte, Phys. Rev. **185**, 509 (1969).

¹⁵P. M. Morse and H. Feshbach, *Methods of Theoretical Physics* (McGraw-Hill, New York, 1953), p. 1575.

¹⁶W. Kohn, Phys. Rev. **84**, 495 (1951).

¹⁷N. W. Ashcroft, Phys. Lett. **23**, 48 (1966); J. Phys. C **1**, 232 (1968).

¹⁸N. W. Ashcroft, in *Soft X-Ray Band Spectra*, edited by D. J. Fabian (Academic, New York, 1968), p. 259.

¹⁹This orbital radius may be directly related to the radius R , introduced by Ashcroft in Ref. 17.

²⁰J. C. Slater, Phys. Rev. **36**, 57 (1930).

²¹G. N. Watson, *Theory of Bessel Functions*, 2nd ed. (Cambridge U. P., Cambridge, England, 1958), p. 363.